Supporting Information

Hierarchical Pore-Engineered Carbon Cathodes for High-Loading, Lean-Electrolyte Lithium–Sulfur Cells

Yu-Hsun Tseng,[a‡] *Tzu-Ching Chan*[a‡] *and Sheng-Heng Chung*[a,*]

[a] Department of Materials Science and Engineering, National Cheng Kung University, No.1, University Road, Tainan City 701401.

Supporting Figures

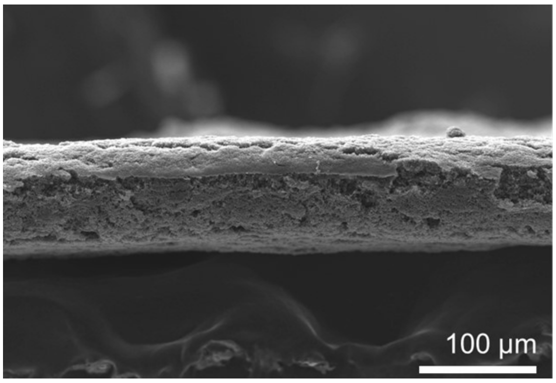

Fig. S1. Cross-sectional SEM inspection of the immersion-precipitation phase-inversion carbon substrate.

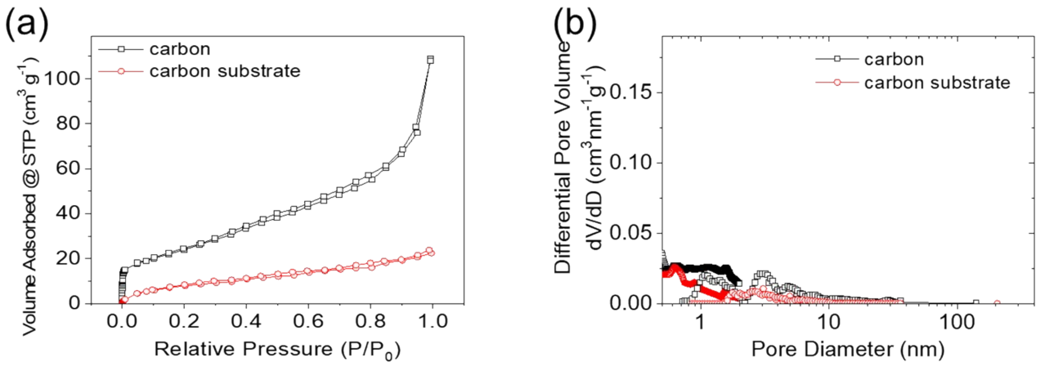

Fig. S2. Porosity analysis of the immersion-precipitation phase-inversion carbon substrate. (a) Nitrogen adsorption-desorption isotherms and (b) pore-size distribution analysis of the raw carbon material and the resulting phase-inversion carbon substrate.

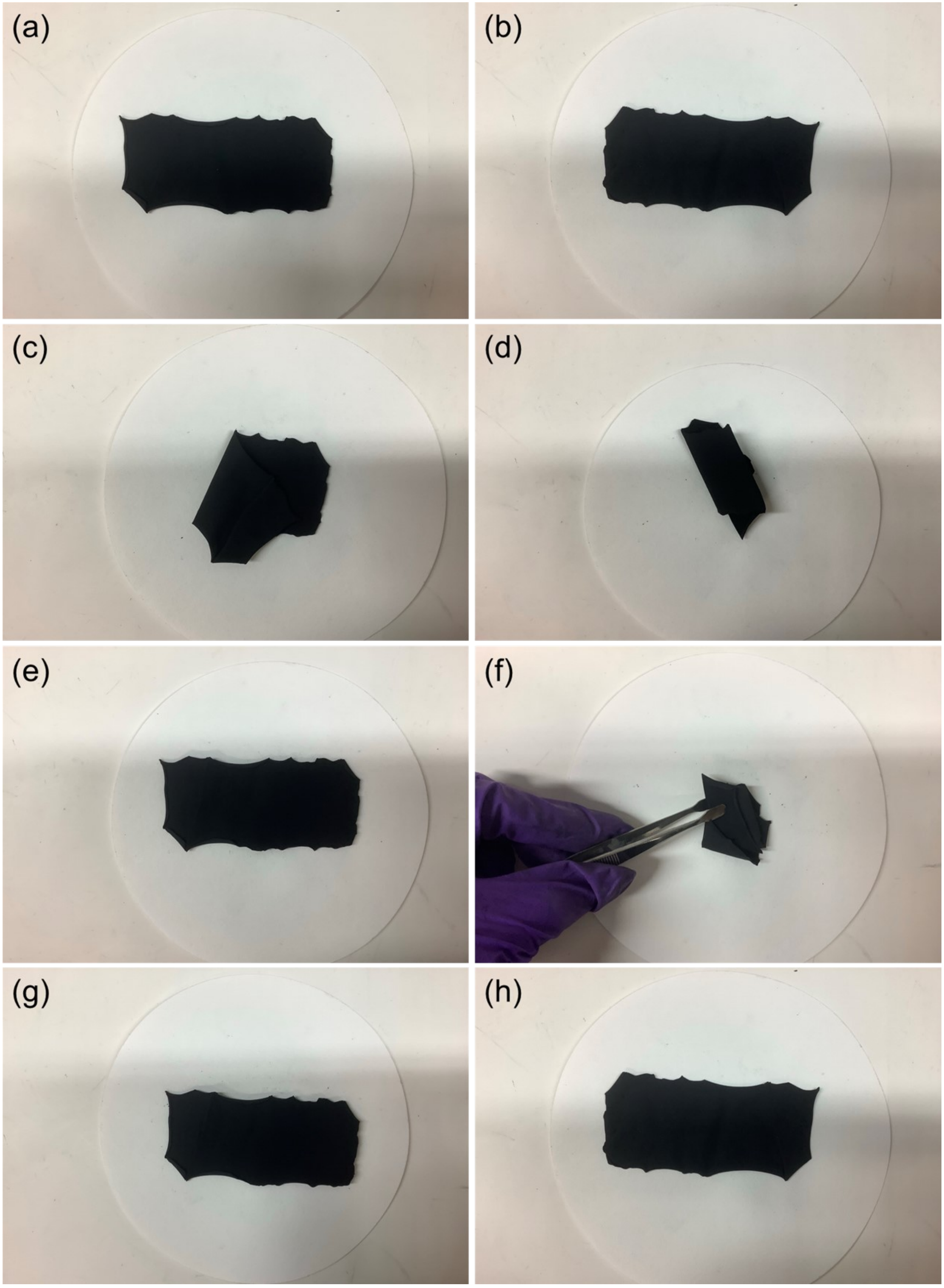

Fig. S3. Digital photographs of the immersion-precipitation phase-inversion carbon substrate. (a) Dense side, (b) porous side, (c) folded sample, (d) rolled sample, (e) recovered sample, (f) kneaded sample, (g) recovered sample of the dense side, and (h) recovered sample of the porous side.

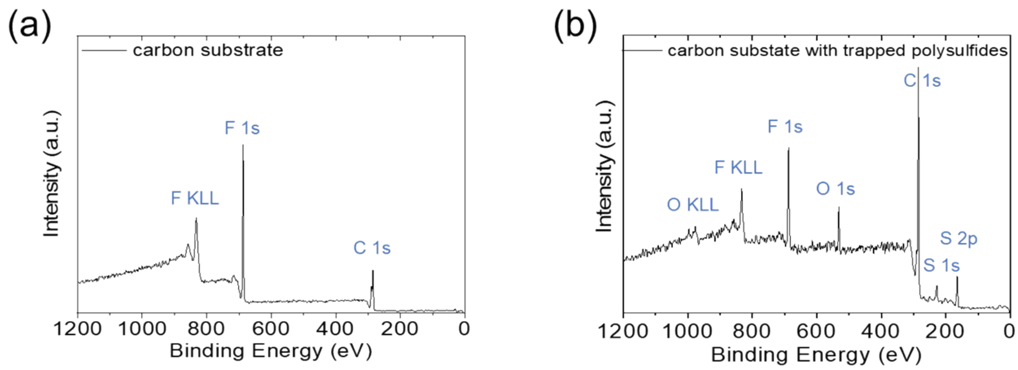

Fig. S4. XPS spectra analysis of the immersion-precipitation phase-inversion carbon substrate. (a) Before and (b) after the polysulfide-trapping analysis.

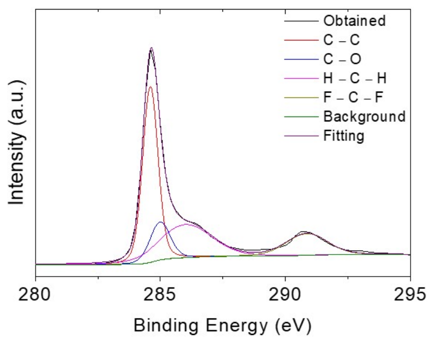

Fig. S5. XPS C1s peak analysis of the immersion-precipitation phase-inversion carbon substrate after the polysulfide-trapping analysis.

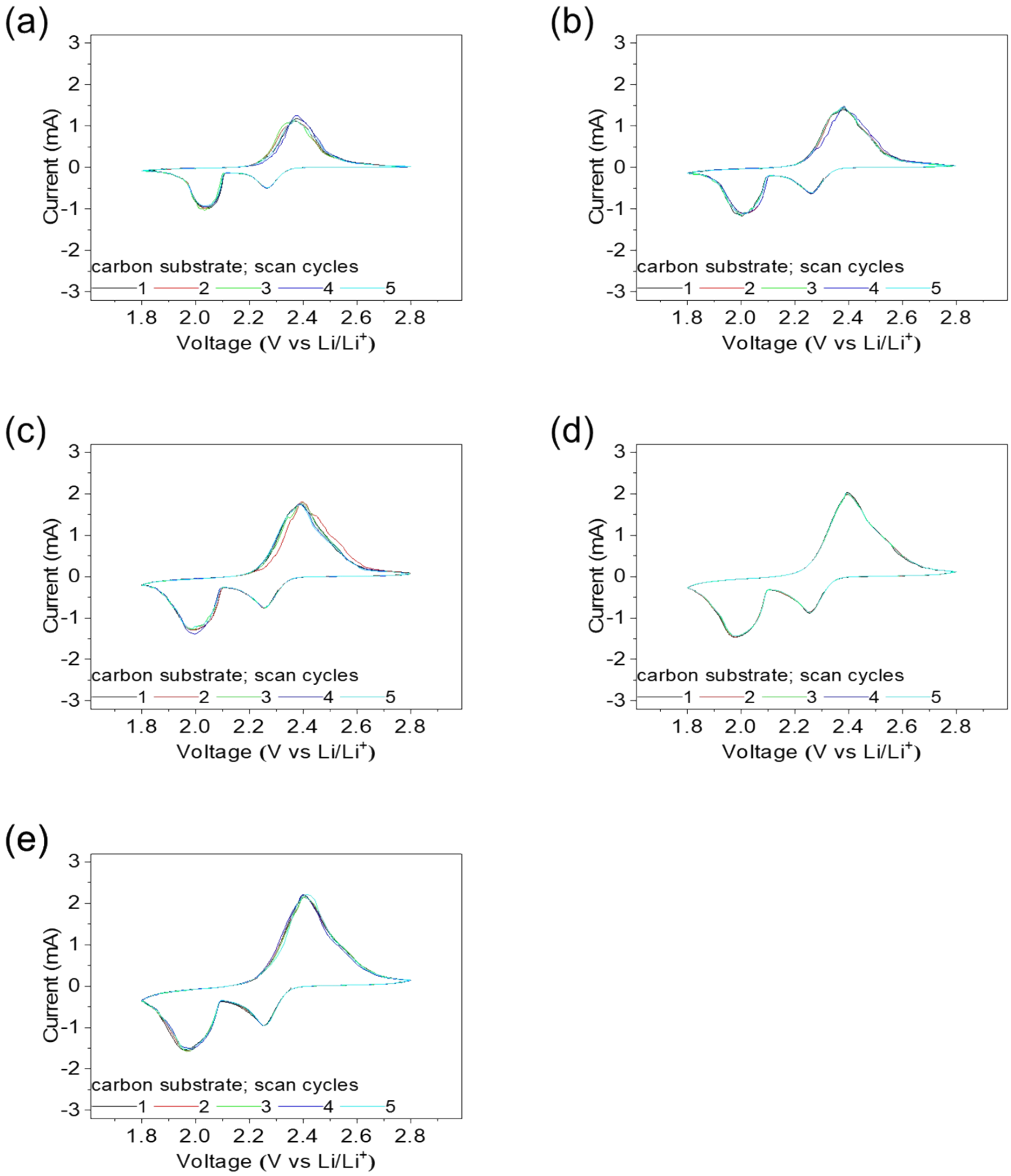

Fig. S6. Rate-dependent CV analysis of the immersion-precipitation phase-inversion cathode. At scan rates of (a) 0.010, (b) 0.015, (c) 0.020, (d) 0.025, and (e) 0.030 mV s^{-1}.

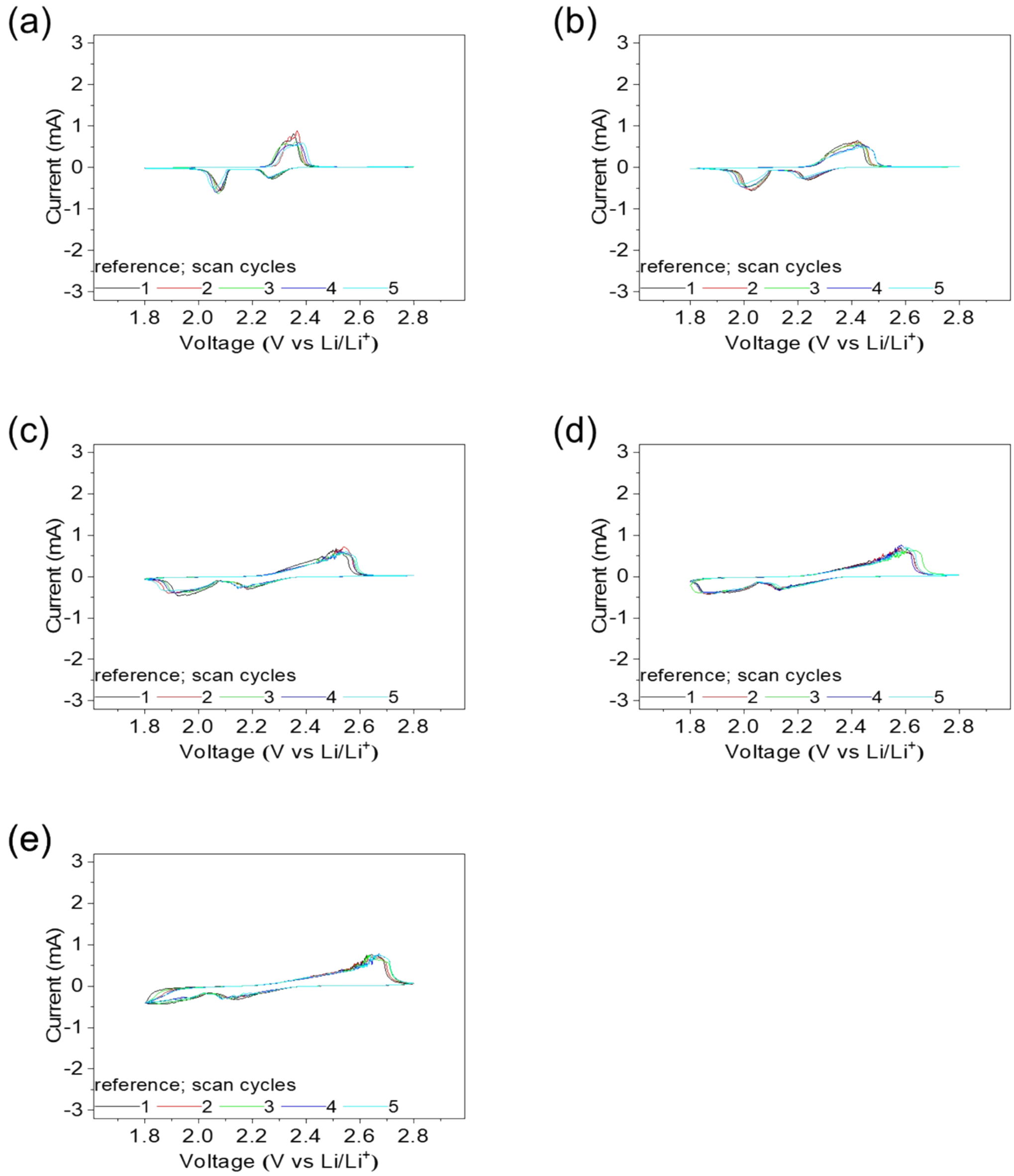

Fig. S7. Rate-dependent CV analysis of a reference cathode. At scan rates of (a) 0.010, (b) 0.015, (c) 0.020, (d) 0.025, and (e) 0.030 mV s^{-1}.

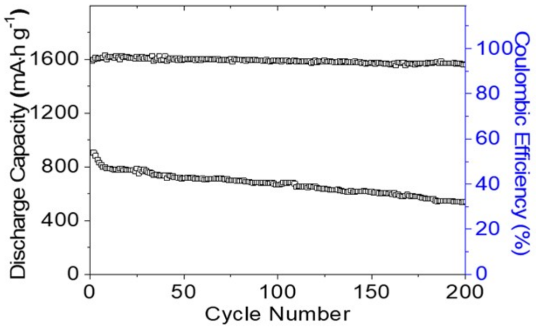

Fig. S8. Long-term cyclability analysis of cells with the immersion-precipitation phase-inversion cathodes using a high sulfur loading of 6 mg cm^{-2} for 200 cycles at a C/20 rate.

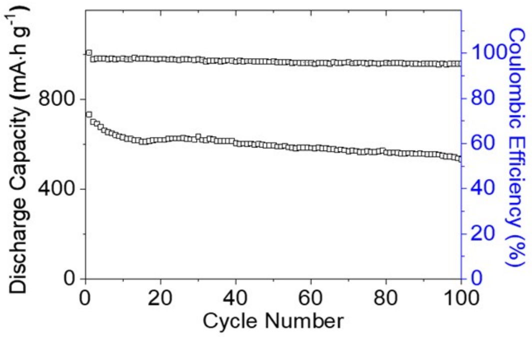

Fig. S9. High-loading capability analysis of cells with the immersion-precipitation phase-inversion cathodes using a high sulfur loading of 8 mg cm^{-2} at a C/10 rate.

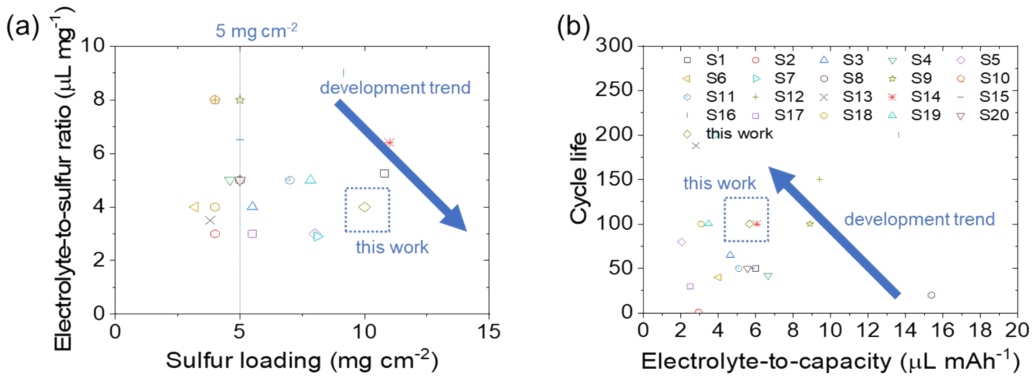

Fig. S10. State-of-the-art development of high-loading sulfur cathodes in lean-electrolyte lithium–sulfur cells reported in this year (2025): (a) sulfur loading and electrolyte-to-sulfur ratio and (b) electrolyte-to-capacity ratio and cycle life.

Supporting Tables

Table S1. State-of-the-art development of high-loading sulfur cathodes in lean-electrolyte lithium–sulfur cells.

i	ii	iii	iv	v	vi	vii	viii	ix	x	xi	xii	xiii
S1	10.8	65	5.2	6.0	800	740	50	93	0.05	8.6	18.0	2025
S2	4.0	63	3.0	2.9	1021		1		0.1	4.1	8.2	2025
S3	5.5	64	4.0	4.6	864	750	65	87	0.1	4.8	9.5	2025
S4	4.6	75	5.0	6.7	751	645	42	86	0.1	3.5	6.9	2025
S5	8.0	64	3.0	2.0	1470	1000	80	68	0.1	11.8	23.5	2025
S6	3.2	72	4.0	4.0	1000	700	40	70	0.1	3.2	6.4	2025
S7	8.1	50	2.9	3.8	757	432	200	57	0.05	6.1	12.3	2025
S8	5.0	64	5.0	15.4	325	225	20	69	0.3	1.6	3.3	2025
S9	5.0	68	8.0	8.9	900	550	100	61	0.2	4.5	9.0	2025
S10	4.0	56	8.0	8.5	945	875	700	93	0.1	3.8	7.6	2025
S11	7.0	63	5.0	5.1	984	590	50	60	0.2	6.9	13.8	2025
S12	4.0	64	8.0	9.4	852	677	150	80	0.2	3.4	6.8	2025
S13	3.8	72	3.5	2.8	1250	700	188	56	1.0	4.8	9.5	2025
S14	11.0	56	6.4	6.1	1055	667	100	63	0.1	11.6	23.2	2025
S15	5.0	60	6.5	5.8	1125	800	50	71	0.1	5.6	11.3	2025

S16	9.2	42	9.0	13.6	659	437	200	66	0.5	6.0	12.1	2025
S17	5.5	70	3.0	2.5	1200	800	30	67	0.1	6.6	13.2	2025
S18	4.0		4.0	3.1	1300	400	100	31	1.0	5.2	10.4	2025
S19	7.8	60	5.0	3.5	1438	830	100	58	0.1	11.3	22.5	2025
S20	5.0	60	5.0	5.6	900	800	50	89		4.5	9.0	2025
this work	10.0	50	4.0	5.6	706	500	100	71	0.1	7.1	14.8	

i: reference number; ii: sulfur loading (mg cm^{-2}); iii: sulfur content (wt%) (our work's sulfur content including the consideration of the total weight of cathode); iv: electrolyte-to-sulfur ratio (μL mg^{-1}); v: electrolyte-to-capacity ratio (μL mAh^{-1}); vi: peak capacity (mAh g^{-1}); vii: reversible capacity at viii cycles (mAh g^{-1}); viii: cycle number; ix: capacity retention (%); x: cycling rate; xi: specific gravimetric capacity per electrode (mAh g^{-1}); xii: energy density (mWh cm^{-2}); xiii: publication year. The references were selected from the first 20 research articles retrieved from Google Scholar using the keywords "high loading," "lean electrolyte," and "lithium–sulfur cells."

Supporting References

S1. C.-C. Wu and S.-H. Chung, *Energy Fuels*, 2025, **39**, 11970–11980.

S2. Y. Fei, M. Li, Z. Li, D. Guan, W. Jia, H. Zhang, K. Amine and G. Li, *Adv. Mater.*, 2025, DOI: 10.1002/adma.202507459.

S3. M. He, L. Zhu, Y. Liu, Y. Jia, Y. Hao, G. Ye, X. Hong, Z. Xiao, Y. Ma, J. Chen, M. B. Shafqat and Q. Pang, *Angew. Chem. Int. Ed.*, 2025, **64**, e202415053.

S4. Q. Qi, F. Shi, J. Yu, Y. Ma, F. Chen, W. Lv, W.-C. Law, S. P. Lau and Z.-L. Xu, *Adv. Sci.*, 2025, **12**, 2410628.

S5. P. Li, Z. Luo, Z. Chen, H. Liu, Y. Liu, J. Guan, J. Jiang, D. Cai, S. Yang and Z. Yang, *Adv. Mater.*, 2025, DOI: 10.1002/adma.202511272.

S6. F. Yang, X. Qi, R. Jiang, X. Jin, Y. Li, F. Zhou, J. Ji, R. Zhang, P. Hu and L. Qiu, *Adv. Funct. Mater.*, 2025, **35**, 241409.

S7. H. Park, J. Lee and C. Yu, *J. Mater. Chem. A*, 2025, **13**, 4452–4459.

S8. L. Lu, N. Kardjilov, X. Meng, K. Dong, Y. Xu, Q. Wu, A. Tengattini, L. Helfen, J. Yang, Y. Guo, M. Exner, I. Manke and Y. Lu, *Adv. Energy Mater.*, 2025, DOI: 10.1002/aenm.202501324.

S9. V. S. Ganesan, S. Nagarajan and L. M. R. Arava, *ACS Appl. Energy Mater.*, 2025, **8**, 2810–2818.

S10. H.-J. Kim, C. Senthil, Y.-C. Kim and H. Y. Jung, *J. Power Sources*, 2025, **656**, 238043.

S11. Z.-X. Chen, J.-J. Zhao, G.-Y. Fang, S. Zhang, J. Ma, M. Zhao, B.-Q. Li and J.-Q. Huang, *Energy Storage Mater.*, 2025, DOI: 10.1016/j.ensm.2025.104502.

S12. K. Liao and A. Manthiram, *Adv. Energy Mater.*, 2025, **15**, 2502062.

S13. H. Cho, J. Jung, I. Kim, J. Kim, S. Kim, J. Hyun, C. H. Lee, H. Kwack, W. Oh, J. Lee and H.-T. Kim, *Nat. Commun.*, 2025, **16**, 6805.

S14. J. Zhang, D. Liang, G. Huang, S. Iqbal, X. Wang, X. Zhu and Y. Zhao, *Small*, 2025, DOI: 10.1002/smll.202507862.

S15. L. Lu, W. Zhang, F. Yan, Y. Xiang, P. Rudolf and Y. Pei, *J. Power Sources*, 2025, **625**, 235689.

S16. Y. Jiang, R. Yang, H. Li, Q. Zhang, X. Dong, H. Shang, J.-H. Ahn, B. Jiang and Y. Yan, *J. Power Sources*, 2025, **650**, 237500.

S17. J. Liu, A. Ghosh, S. Kondou, S. Li, K. Ueno, K. Dokko and M. Watanabe, *ACS Appl. Energy Mater.*, 2025, **8**, 1570–1579.

S18. K. M. Le, A. Phan, C. Anderson, S. Feng, N. T. Tran, L. Shi, M. V. Duong, S. Parab, B. Bhamwala, W. Bao, Y. S. Meng, J. Xiao, J. Liu, D. Lu and P. M. L. Le, *ACS Appl. Energy Mater.*, 2025, **8**, 9663–9670.

S19. X. Feng, X. Ren, H. Tian, M. Cui, G. Lu, J. Zhang and X. Gao, *J. Am. Chem. Soc.*, 2025, **147**, 30042–30049.

S20. H. Li, Z. Huang, P. Qian, Y. Wang, R. Gao, A. Bendounan, H. Wang, Z. Chen, H. Zeng and G. Li, *Adv. Funct. Mater.*, 2025, **35**, 2419837.